



## TIGIT/PVR and LncRNA ANRIL dual-targetable PAMAM polymeric nanoparticles efficiently inhibited the hepatoma carcinoma by combination of immunotherapy and gene therapy

Tianyin Wang, Peiting Li, Tao Wan, Biao Tu, Jing Li & Feizhou Huang

To cite this article: Tianyin Wang, Peiting Li, Tao Wan, Biao Tu, Jing Li & Feizhou Huang (2021): TIGIT/PVR and LncRNA ANRIL dual-targetable PAMAM polymeric nanoparticles efficiently inhibited the hepatoma carcinoma by combination of immunotherapy and gene therapy, Journal of Drug Targeting, DOI: [10.1080/1061186X.2021.1879088](https://doi.org/10.1080/1061186X.2021.1879088)

To link to this article: <https://doi.org/10.1080/1061186X.2021.1879088>



Published online: 10 Feb 2021.



Submit your article to this journal [↗](#)



Article views: 47



View related articles [↗](#)



View Crossmark data [↗](#)

# TIGIT/PVR and LncRNA ANRIL dual-targetable PAMAM polymeric nanoparticles efficiently inhibited the hepatoma carcinoma by combination of immunotherapy and gene therapy

Tianyin Wang<sup>a</sup>, Peiting Li<sup>b</sup>, Tao Wan<sup>a</sup>, Biao Tu<sup>a</sup>, Jing Li<sup>a</sup> and Feizhou Huang<sup>a</sup>

<sup>a</sup>Department of Hepatopancreatobiliary Surgery, Third Xiangya Hospital, Central South University, Changsha, Hunan, China; <sup>b</sup>Department of Breast Thyroid Surgery, Third Xiangya Hospital, Central South University, Changsha, Hunan, China

## ABSTRACT

Herein, a novel polymeric nanoparticle was designed to inhibit hepatoma carcinoma by simultaneously targeting the T cell immunoreceptor with Ig and ITIM domains (TIGIT)/poliovirus receptor (PVR) and long noncoding RNAs antisense noncoding RNA in the INK4 locus (LncRNA ANRIL). Firstly, the siANRIL-loaded nanoparticles (NP-siANRIL) was developed by methoxy-poly (ethylene glycol)-polyamidoamine (mPEG-PAMAM) and polyamidoamine-poly (ethylene glycol)-disulphide bond-carboxyl (PAMAM-PEG-S<sub>2</sub>-COOH) using the self-assembly method. Then the <sup>D</sup>TBP-3 peptide, a newly developed identified peptide which could occupy the binding interface and effectively block the interaction of TIGIT with its ligand PVR, was further conjugated on the surface of NP-siANRIL *via* the glutathione (GSH)-sensitive disulphide linkage. In this way, the binding ability of <sup>D</sup>TBP-3 to TIGIT was remained once they were entrapped into the tumour tissues which were abundant of GSH. The present study demonstrated that <sup>D</sup>TBP-3NP-siANRIL exhibited an excellent anti-tumour effect on hepatoma carcinoma *in vivo* by simultaneously inhibited the expression of miR-203a and its downstream genes and increased the percentages of NK cells and T cells. In a word, the present study has presented a novel strategy for treatment of hepatoma carcinoma by simultaneously targeting of TIGIT/PVR and LncRNA ANRIL.

## ARTICLE HISTORY

Received 16 November 2020  
Revised 17 January 2021  
Accepted 18 January 2021

## KEYWORDS

Hepatoma carcinoma;  
glutathione; TIGIT; ANRIL;  
immunotherapy

## Introduction

Hepatocellular carcinoma (HCC), also known as liver cancer, is one of the malignant tumours that seriously threaten human life. It is the fifth most common malignant tumour and ranks third among the causes of cancer deaths worldwide [1,2]. There are about 1 million people expected to die from HCC yearly. Due to the lack of accurate and timely early diagnosis to differentiate HCC from cirrhosis, a sharp increase in HCC patients was induced [3]. Metastasis and recurrence of HCC are the main causes of death and also are the greatest challenge for clinical treatment and prevention of HCC [4].

Long noncoding RNAs (lncRNAs) are novel identified noncoding RNAs with more than 200 nucleotides in length, participating in physiological activity in nuclear or cytoplasmic compartments [5,6]. lncRNA is a type of epigenetic modulation that refers to transcription and posttranscription regulation [6]. Accumulating evidence has revealed that numerous lncRNAs participate in tumour genesis and biological processes, such as proliferation, invasion, metastasis, and apoptosis [7,8]. The aberrant expression levels of lncRNAs have the potential to act as biomarkers for tumour prediction [9]. ANRIL is transcribed as a 3.8 kb lncRNA with a large germline deletion in the CDKN2A/B (also known as INK4B-ARF-INK4A) gene cluster [10]. Previous studies have demonstrated that ANRIL was upregulated in tumour tissue and function as a tumour-promoting lncRNA in a number of malignancies, such as nasopharyngeal carcinoma, lung cancer, and multiple myeloma [11–13]. Additionally, ANRIL was highly expressed in HCC tissues,

and its expression was associated with histologic grade and Tumour Node Metastasis (TNM) stage of HCC patients [14], indicating ANRIL may serve as an efficient clinical biomarker for HCC patients.

Besides the aberrant expression of lncRNAs, immune checkpoints such as the PD-1/PD-L1 which leads to the exhaustion of immune cells and immune escape of cancer plays significant role in tumour progress [15,16]. Blockade of the PD-1/PD-L1 can normalise cancer immunity in the tumour microenvironment, and constitute a revolution in cancer immunotherapy [17]. However, the therapeutic effects of PD-1/PD-L1 blockade are limited (<30% response rates), and adaptive resistance is often observed [18]. Therefore, potent and efficacious targets are urgently needed. TIGIT is a novel immune checkpoint molecule expressed on NK and T cells, which competes with costimulatory receptor CD226 for the shared ligand PVR to deliver immunosuppressing signals [19,20]. Previous study demonstrated that the TIGIT was expressed higher than PD-1 in many tumours especially anti-PD-1 resistant tumours [21]. Based on this, the TIGIT could be acted as a new checkpoint receptor targets for cancer immunotherapy. <sup>D</sup>TBP-3 is a newly developed peptide which could occupy the binding interface and effectively block the interaction of TIGIT with its ligand PVR [21]. <sup>D</sup>TBP-3 showed proteolytic resistance, tumour tissue penetrating ability, and significant tumour suppressing effects in a CD8<sup>+</sup> T cell dependent manner [21]. More importantly, <sup>D</sup>TBP-3 could inhibit tumour growth and metastasis in antiPD-1 resistant tumour model [21].

Polymeric nanoparticles are solid, biodegradable, and colloidal systems that have been widely used as drug vesicles for delivery of siRNAs [22]. However, the low charge density and stiff backbone structure have led to inconsistencies in encapsulation efficiency of those siRNAs [23]. PAMAM has been one of the most promising candidate natural polymers for siRNA delivery due to its high encapsulation efficiency, relatively low toxicity and high transfection efficiency [24]. Furthermore, PEGylation of the PAMAM led to a significant prolonged circulation time in blood [25]. Previous study demonstrated that the encapsulation efficiency of the PAMAM-based nanoparticles was more than 95%, indicating an excellent siRNA loading capability [26]. Therefore, in the present study, the PEG-PAMAM was selected as the polymer carrier and prepared for siRNA-loaded nanoparticles (NP-siANRIL).

Moreover, to simultaneously blocks the TIGIT/PVR for immunotherapy, the TIGIT-targeting peptide <sup>D</sup>TBP-3 was further covalently conjugated on the surface of NP-siANRIL. Importantly, the <sup>D</sup>TBP-3 peptides were conjugated on the NP-siANRIL *via* the GSH-sensitive disulphide linkage to remain the blocking effect of <sup>D</sup>TBP-3. It was previously reported that the GSH levels in the intracellular compartment was  $2\text{--}10 \times 10^{-3}$  M while in the extracellular microenvironment was  $2\text{--}20 \times 10^{-6}$  M [27]. Such different GSH levels indicated that the conjugated <sup>D</sup>TBP-3 peptides could be completely released in tumour cells and keep structural integrity under the normal physiological conditions. In a word, the present study has presented a novel strategy for treatment of hepatoma carcinoma by simultaneously targeting of TIGIT/PVR and LncRNA ANRIL.

## Materials and methods

### Chemical agents

The mPEG<sub>3400</sub>-PAMAM<sub>30,000</sub>, PAMAM<sub>30,000</sub>-PEG<sub>3000</sub>-S<sub>2</sub>-COOH, and the DiR (1, 10-dioctadecyl-3, 3, 30, 30-tetramethyl indotricarbocyanine iodide)-labeled polymers were purchased from Laysan Bio (St. Louis, MO, USA). 1-(3-(dimethylamino)propyl)-3-ethylcarbodiimide (EDC) and *N*-hydroxy-succinimide (NHS) were purchased from Sigma-Aldrich (USA). The <sup>D</sup>TBP-3 peptide with sequence of GGYTFHWHRLNP-NH<sub>2</sub> was synthesised by China Peptides Co., Ltd. (Shanghai, China). The siRNA pcDNA3.1-ANRIL (siANRIL) with primer sequence of 5'-GGUCAUCUCAUUGCUCUAU-3', miR-203a mimic and Fluorescein Isothiocyanate (FITC)-conjugated siANRIL used in the cell uptake assays taken from Thermo Fisher Scientific (Germany). 3-(4,5-dimethyl-2-thiazolyl)-2,5-diphenyl-2-H-tetrazolium bromide (MTT) assay kit was from Roche (Roche Applied Science, Mannheim, Germany). DAPI All of the other chemicals were analytical or reagent grade and were acquired from Sinopharm Chemical Reagent Co., Ltd (Shanghai, China) unless specified otherwise.

### Cell culture and animals

The HCC cell lines, Hep3B, were obtained from Shanghai Institute of Biochemistry and Cell Biology (China). The cells were cultured in RPMI 1640 medium supplemented with 10% foetal bovine serum (FBS) (Gibco, Grand Island, NY) in a humidified chamber with 5% CO<sub>2</sub> at 37 °C.

The Six-week-old BALB/c mice were obtained from the Sino-British Sippr/BK Lab Animal Ltd. (Shanghai, China). For establishment of tumour-bearing mice models,  $5 \times 10^5$  Hep3B cells in 100 μL phosphate buffer (PBS, 0.01 M, pH 7.4) was intravenously inoculated into the right flank of the mouse. Then the tumour-

bearing mice were raised at a constant temperature with free access to food and water.

### Preparation and characterisation of the polymer/siRNA nanoparticles

To prepare the polymer/siRNA nanoparticles (NP-siANRIL), 16 mg of PAMAM-PEG-S<sub>2</sub>-COOH and 4 mg of mPEG-PAMAM was dissolved by DEPC-treated water, respectively, then mixed with siRNA at the N/P ratio of 10:1. After that, the mixture was immediately vortexed for 30 s and incubated for 30 min at 25 °C to ensure complete complexation. For conjugation of <sup>D</sup>TBP-3 peptides, the developed NP-siANRIL was dissolved with PBS containing EDC (200 mM) and NHS (100 mM) followed by incubation with <sup>D</sup>TBP-3 peptides for 6 h. Then the formed <sup>D</sup>TBP-3NP-siANRIL was collected by centrifugation at 14,000 rpm for 1 h. The FITC or DiR-labeled nanoparticles were developed using the same methods as above besides the siANRIL was replaced with the FITC-labeled siANRIL or the polymers were replaced with the DiR-labeled polymers.

Particle size and zeta-potential of the formed <sup>D</sup>TBP-3NP-siANRIL were determined by the dynamic light scattering technique (DLS) on a Zetasizer Nano ZS (Malvern Instruments, Ltd., UK). The morphology of <sup>D</sup>TBP-3NP-siANRIL was examined under the transmission electron microscope (TEM) (JEM-1230, JEOL). High Performance Liquid Chromatography (HPLC) analysis was applied to investigate the peptides conjugation efficiency.

### Sensitivity of <sup>D</sup>TBP-3NP-siANRIL to GSH *in vitro*

The sensitivity of <sup>D</sup>TBP-3NP-siANRIL to GSH was examined by study of <sup>D</sup>TBP-3 release from <sup>D</sup>TBP-3NP-siANRIL in the medium of GSH *in vitro*. In brief, 20 mg of <sup>D</sup>TBP-3NP-siANRIL were dissolved by 1 ml PBS and subjected into a dialysis bag (MWCO 8000 Da, Greenbird Inc., Shanghai, China). Then the samples were incubated in 50 ml PBS containing 5 mM GSH at 37 °C with a shaking speed of 100 rpm. At predetermined time points, 200 μL samples were withdrawn and immediately supplemented with equal volumes of fresh release medium. The obtained samples were finally analysed by HPLC method.

### Stability of <sup>D</sup>TBP-3NP-siANRIL

The stability of <sup>D</sup>TBP-3NP-siANRIL was investigated in the medium of isotonic saline solution containing 5% (w/v) human serum albumin which was similar to the main compositions of human plasma. <sup>D</sup>TBP-3NP-siANRIL was dispersed in the medium at concentrations of 100 μg/mL followed by incubation at 37 °C. Then the particle size of <sup>D</sup>TBP-3NP-siANRIL was determined at predetermined time points ( $n = 3$ ) using the Malvern Zetasizer.

### Hepatoma carcinoma targeting assay

The hepatoma carcinoma targeting ability of <sup>D</sup>TBP-3NP-siANRIL was respectively determined by *in vitro* cell uptake assay and *in vivo* tumour targeting assay. For cell uptake study,  $1 \times 10^4$  Hep3B cells were seeded in 24-well plates and incubated for 24 h. Then the cells were respectively incubated with different concentrations (10 μg/mL and 100 μg/mL) of FITC-labeled <sup>D</sup>TBP-3NP-siANRIL and NP-siANRIL. For qualitative analysis, after 24 h co-incubation, the cells were washed with PBS and fixed with 4% paraformaldehyde followed by observation using the fluorescent microscope (Leica DMI 4000B, Germany). For quantitative evaluation, the cell

after treatment for 24 h was collected and the fluorescence intensity of the cells was measured by the flow cytometer (FACS Calibur, BD, USA).

For *in vivo* tumour targeting assay, six tumour-bearing mice were randomly grouped ( $n = 3$ ) and respectively injected with DiR-labeled NP-siANRIL and  $^{125}\text{I}$ -TBP-3NP-siANRIL. After 24 h, the mice in each group were euthanised followed by collection of tumour tissues and primary organs, including heart, liver, spleen, lung, and kidney. For quantitative analysis of bio-distribution, the obtained tumour tissues and primary organs were homogenated. Then HPLC analysis was finally performed for determining levels of DiR.

### Anti-proliferation assay

The anti-proliferation of  $^{125}\text{I}$ -TBP-3NP-siANRIL on Hep3B cells was evaluated by the MTT experiments.  $5 \times 10^3$  Hep3B cells were seeded in 96-well plates and incubated for 24 h. Then the cells were respectively treated with pcDNA3.1-siANRIL, NP-siANRIL,  $^{125}\text{I}$ -TBP-3NP, and  $^{125}\text{I}$ -TBP-3NP-siANRIL. After 48 h of incubation, 20  $\mu\text{L}$  of MTT (5 mg/mL) was added into each well followed by incubation for 4 h. Then the formed formazan crystals were dissolved by 150  $\mu\text{L}$  of DMSO. Cell viability was finally determined using the microplate reader (Thermo Multiskan MK3).

### Cell apoptosis assay

The AnnexinV-FITC/PI double staining kit was applied to evaluate the ability of  $^{125}\text{I}$ -TBP-3NP-siANRIL to induce cell apoptosis.  $1 \times 10^4$  Hep3B cells were seeded in 24-well plates and incubated for 24 h. Then the cells were respectively treated with pcDNA3.1-siANRIL, NP-siANRIL,  $^{125}\text{I}$ -TBP-3NP, and  $^{125}\text{I}$ -TBP-3NP-siANRIL. After 24 h of incubation, the cells in each well were collected and resuspended in 200  $\mu\text{L}$  binding buffer for double staining with Annexin V-FITC (5  $\mu\text{L}$ ) and PI (10  $\mu\text{L}$ ) in accordance with the manufacturer's protocol. Finally the cell apoptosis rate was determined using the flow cytometer.

### Cell migration

The lateral migration and vertical mobility of Hep3B cells were respectively investigated by wound healing assay and trans-well assay. For investigation,  $1 \times 10^5$  Hep3B cells were seeded in 24-well plates followed by culturing to 90% confluence in complete medium. Then the wounded lines across the centre of each well were formed using the plastic pipette tip (1 mm). After washed with PBS to remove the untouched cell debris, the residual cells were respectively treated with pcDNA3.1-siANRIL, NP-siANRIL,  $^{125}\text{I}$ -TBP-3NP, and  $^{125}\text{I}$ -TBP-3NP-siANRIL for 24 h. Then the images of cell migration into the wound surface were obtained using the inverted microscope and the wound healing rate was calculated using the Image J software.

The trans-well assay was performed by incubation of  $1 \times 10^5$  cells in the top chamber of 24-well trans-well with the lower chamber contained culture medium with 10% FBS served as a chemoattractant. After 24 h of incubation with the above formulations, the migrated cells were fixed and stained with crystal violet solution. After 30 min of incubation, the stained cells were photographed under the phasecontrast microscopy.

### Anti-tumour effect *in vivo*

Forty tumour-bearing mice were randomly grouped ( $n = 10$ ) and respectively injected with Saline (using as the control group), pcDNA3.1-siANRIL, NP-siANRIL,  $^{125}\text{I}$ -TBP-3NP, and  $^{125}\text{I}$ -TBP-3NP-siANRIL. Then the tumour growth was carefully observed every three days in three weeks. Besides, the survival time of each mice in each group was recorded and analysed by Kaplan–Meier survival curve. For TUNEL and immunohistochemical analysis, the obtained tumour tissues were fixed with 10% neutral buffered formalin for 48 h followed by immersion in paraffin. After that, 5  $\mu\text{m}$  tumour tissue sections were prepared for Tdt-mediated dUTP nick-end labelling (TUNEL) analysis and routine haematoxylin and eosin (H&E) staining.

### Western blot assay

At the end of tumour experiments, all tumour tissues were obtained for homogenate. Total protein in tumour tissues was collected and the concentration was determined by BCA assay. Then they were separated by 10% SDS-PAGE followed by transfection to PVDF membrane. After blocking with 5% milk at room temperature for 1 h, the samples were incubated with primary antibodies against EGFR (1:1500), p-AKT (1:1500), ERK (1:1500), and Bcl-2 (1:1500) at 4 °C for 1 h. After washing with PBST, the horseradish peroxidase conjugated IgG (1:3000) was added and incubated for 24 h. Finally, the samples were analysed using the ECL kit (Merck Millipore, Billerica, MA, USA) with  $\beta$ -actin as the internal reference.

### Real time-qPCR assay

After the obtained tumour tissues were homogenated, total RNAs were extracted using using the TRizol (Invitrogen, Thermo Fisher Scientific). The expression of various genes was detected using the miScript Reverse Transcription Kit (Qiagen NV, Venlo, Netherlands) and ABI 7500 PCR analyser (Applied Biosystems, Thermo Fisher Scientific). The reaction conditions were initial denaturation at 93 °C for 1 min, followed by 40 cycles of denaturation at 93 °C for 30 s, annealing at 65 °C for 30 s, and extension at 72 °C for 10 min, and final extension at 72 °C for 5 min. Then the  $2^{-\Delta\Delta\text{Ct}}$  method was applied for analysis with the GAPDH used for normalising the gene expression, and U6 was used for normalising miR-203a expression.

### Statistical analysis

Graphed prism software (version 7.0) was used for statistical analysis. Data are expressed as mean  $\pm$  SD. Differences between groups were evaluated by one-way analysis of variance.  $p < .05$  was considered significantly different.

## Results and discussion

### The expression of lncRNA ANRIL and TIGIT in hepatoma carcinoma

As the member of lncRNAs, ANRIL has been reported was associated with progress of various cancer types, such as the osteosarcoma, lung cancer, and hepatocellular carcinoma [12,28,29]. Previous study revealed that ANRIL plays significant role in the promotion of hepatocellular carcinoma progress and knockdown of ANRIL contributed to obvious suppression of cell proliferation

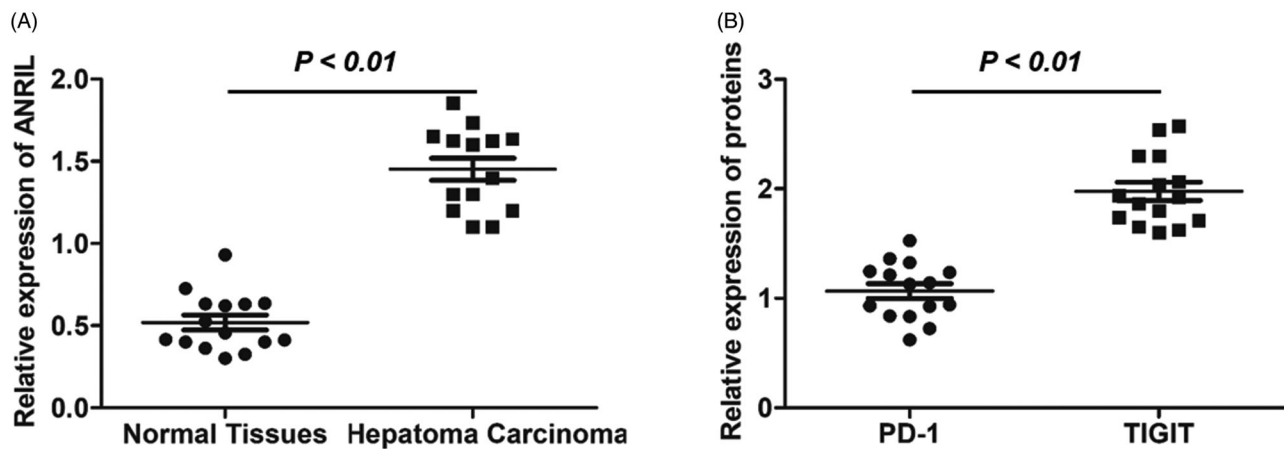


**Figure 1.** Expression of lncRNA ANRIL and TIGIT in hepatoma carcinoma detected by the RT-qPCR experiments. (A) Higher level of lncRNA ANRIL was detected in hepatoma carcinoma than normal tissue. (B) The signal of TIGIT in hepatoma carcinoma was obviously stronger than the PD-1.  $p < .01$ , significantly different from the control group.

and invasion [29]. In the present study, it was confirmed that there was an obvious increase of ANRIL level in hepatoma carcinoma when compared with normal tissue (Figure 1(A)). Additionally, detection of TIGIT revealed that higher expression of TIGIT than PD-1 was observed in hepatoma carcinoma (Figure 1(B)).

#### Physicochemical characterisation of the $^D$ TBP-3NP-siANRIL

Delivery of drugs to the tumours by nanoparticles is impacted by multiple factors such as size, shape, surface charge, surface chemistry (PEGylation, ligand conjugation) and compositions [30,31]. As one of the most crucial parameters, particle size plays pivotal role in the circulation time and tumour accumulation [31]. It was previously reported that the polymer nano-drug delivery system which near 100 nm in diameter tend to represent an optimal range for leveraging the EPR effect and minimising clearance [31]. In our study, the developed  $^D$ TBP-3NP-siANRIL has an average diameter of 101.23 nm (Figure 2(A)), which was slightly higher than the  $^D$ TBP-3 un-conjugated NP-siANRIL (93.56 nm). The  $^D$ TBP-3 conjugation efficiency was approximately 94% as demonstrated by HPLC analysis, the morphology of  $^D$ TBP-3NP-siANRIL was subsequently detected using the TEM and presented a nearly spherical appearance (Figure 2(B)). Moreover, it was previously reported that nearly neutral particles (zeta-potential of  $-10$  to  $10$  mV) are easier to avoid opsonised and Kupffer cells clearance and distribute deeply and homogeneously in tumour [30,31]. The developed  $^D$ TBP-3NP-siANRIL exhibited an average zeta-potential of 8.23 mV. In this study, the PEG-PAMAM was selected as the polymer carrier and prepared for siRNA-loaded nanoparticles due to its high encapsulation efficiency [24]. The results demonstrated that the encapsulation efficiency of the developed  $^D$ TBP-3NP-siANRIL was more than 96%, indicating an excellent siRNA loading capability.

In the present study, the  $^D$ TBP-3 peptide was covalently conjugated on the surface of NP-siANRIL via a GSH-sensitive linkage. In this case, the  $^D$ TBP-3 peptide could be completely released to bind the TIGIT for blocking of TIGIT/PVR. To verification whether the  $^D$ TBP-3 peptide could release from  $^D$ TBP-3NP-siANRIL in tumour, an *in vitro* release assay was conducted in the medium containing 5 mM GSH which was consistent with concentrations in tumour tissues [27]. As demonstrated in Figure 2(C), negligible release signal of  $^D$ TBP-3 peptide was detected in the medium

without GSH. However, in the medium containing 5 mM GSH, nearly 100% of  $^D$ TBP-3 peptides were released within 6 h. These results indicated the developed  $^D$ TBP-3NP-siANRIL possessed satisfactory structure stability under normal physiology condition but sensitive enough after they were entrapped into tumour site.

#### Stability investigation *in vitro*

Besides the physicochemical properties, various substances in plasma also exerted austere challenge to the nanoparticle drug delivery to tumour [31]. Therefore, enough stability is essential for nano-drug delivery system to reach tumour site and finally release the active agent to induce pharmacological effect [31]. To investigate the stability of  $^D$ TBP-3NP-siANRIL, it was incubated in the medium of PBS containing 10% rat plasma followed by detection of the particle size changes. As demonstrated in Figure 2(D), after incubation for 72 h, the particle size of  $^D$ TBP-3NP-siANRIL was slightly increased to 109.23 nm while particle size of NP-siANRIL was slightly increased to 102.23 nm. These results indicated the developed  $^D$ TBP-3NP-siANRIL has a relative satisfactory stability of particle size and decoration of  $^D$ TBP-3 peptides exerted negligible effect.

#### Tumour targeting *in vitro* and *in vivo*

The tumour targeting ability of  $^D$ TBP-3NP-siANRIL was respectively determined by *in vitro* cellular experiments and *in vivo* mice model assay. As shown in Figure 3(A,B), cellular up-take of  $^D$ TBP-3NP-siANRIL and NP-siANRIL displayed a similar behaviour and was concentration-dependent. Moreover, the fluorescent signal in the  $^D$ TBP-3NP-siANRIL treated cells was similar to the NP-siANRIL treated cells, indicated the  $^D$ TBP-3-conjugated nanoparticles have no more advantages in mediating tumour cell uptake than the un-conjugated ones. However, *in vivo* tumour targeting assay revealed that the  $^D$ TBP-3-conjugated  $^D$ TBP-3NP-siANRIL resulted in dramatically higher accumulation of nanoparticles in tumour sites than the NP-siANRIL (Figure 3(C,D)). Such contrast results were mainly ascribed to that the immune checkpoint TIGIT was highly expressed on memory T cells, follicular helper T cells, regulatory T cells and NK cells while not tumour cells [21]. Therefore, the developed  $^D$ TBP-3NP-siANRIL has excellent ability to targeting delivery of drugs to tumours but not tumour cells.

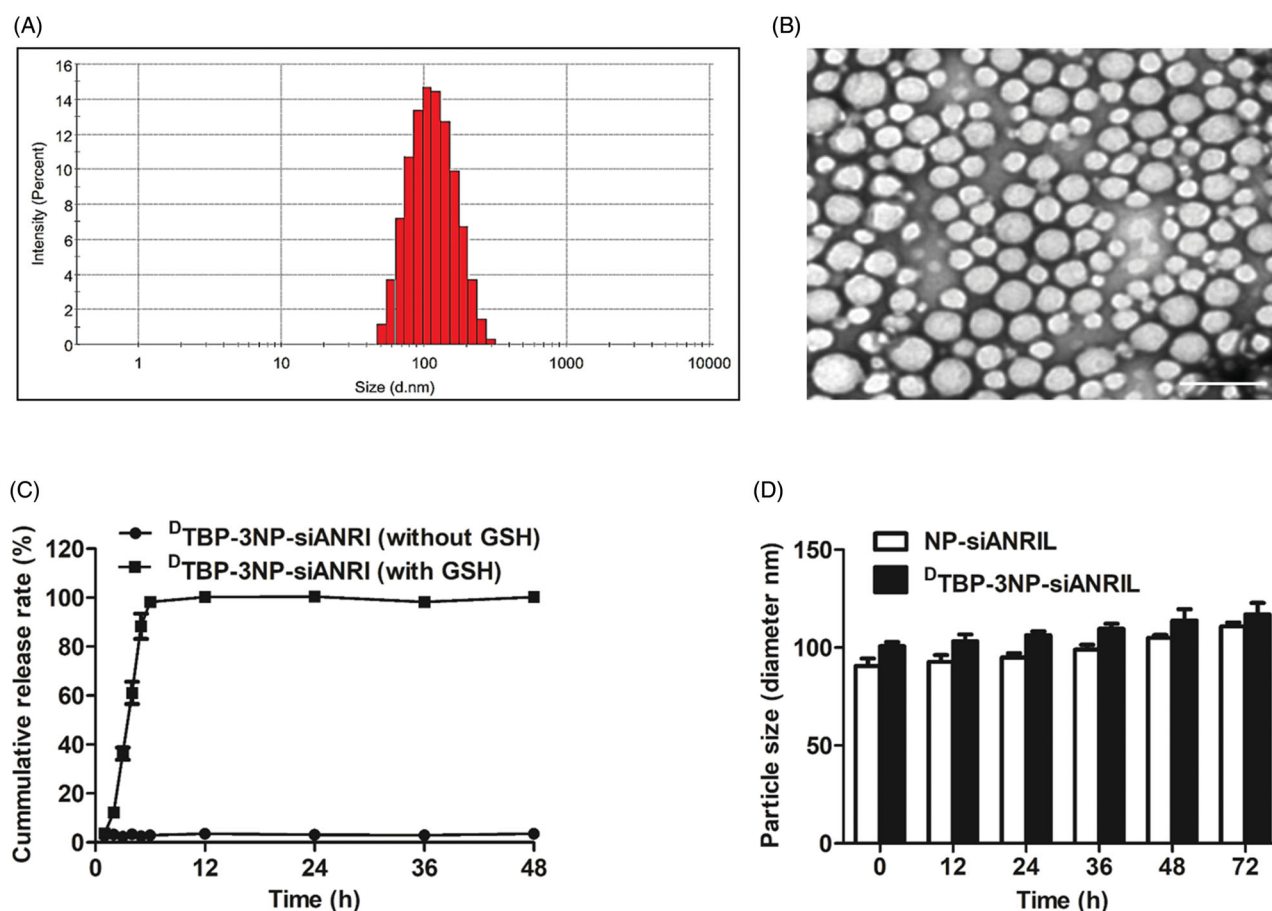


**Figure 2.** Physicochemical characterisation of the  $^{D13}$ TBP-3NP-siANRIL. (A) Particle size of  $^{D13}$ TBP-3NP-siANRIL determined by the DLS analysis. (B) Morphology of  $^{D13}$ TBP-3NP-siANRIL observed under the TEM. (C) Cumulative release rate (%) of  $^{D13}$ TBP-3 from the  $^{D13}$ TBP-3NP-siANRIL in the release medium of PBS containing 10 mM GSH and 0 mM GSH, respectively. (D) Particle size changes of  $^{D13}$ TBP-3NP-siANRIL and NP-siANRIL during 72 h of incubation in the medium of PBS containing 10% plasma.

#### Anti-tumour effect of $^{D13}$ TBP-3NP-siANRIL

Anti-tumour effect  $^{D13}$ TBP-3NP-siANRIL was also evaluated both at cellular level and tumour-bearing animal model. As shown in Figure 4(A–C), the cells transfected with siANRIL exhibited lower cell viability, higher apoptosis rate, and slower migration rate than the control cells, confirmed the favourable role of ANRIL in promotion of hepatoma carcinoma cells. Moreover, the silencing efficacy of siANRIL was further signally enhanced after it was delivered by the nanoparticles, indicated a super transfection efficacy of NP-siANRIL than the free siANRIL. Besides, similar to the cellular uptake assay, there was no significant difference between the group of NP-siANRIL and  $^{D13}$ TBP-3NP-siANRIL due to barren expression of TIGIT on hepatoma carcinoma cells. However, *in vivo* anti-tumour experiments displayed that the tumour-bearing mice treated by  $^{D13}$ TBP-3NP-siANRIL exhibited an obvious slower tumour growth rate and resulted in longer survival time than the mice treated by NP-siANRIL. Further TUNEL and immunohistochemical analysis revealed that the tumours in the group of  $^{D13}$ TBP-3NP-siANRIL have the largest area of cell apoptosis rate and the lowest expression of TIGIT than other groups. The role of  $^{D13}$ TBP-3 peptide in regulation of hepatoma carcinoma growth was investigated as well. Similar to above, there was no obvious anti-tumour effect was observed for  $^{D13}$ TBP-3 on Hep3B cells. However, it was demonstrated that treatment of hepatoma carcinoma-bearing mice with  $^{D13}$ TBP-3NP contributed to a significant slower tumour growth rate and longer survival time than control group, suggesting a relative excellent anti-tumour ability for  $^{D13}$ TBP-3 *in vivo*.

#### Influence of $^{D13}$ TBP-3NP-siANRIL on cellular signalling and immunity

The role of lncRNAs in tumorigenesis and tumour progress was mainly through regulating the expression of various genes [12, 29]. Previous study revealed that ANRIL promoted the progress of glioma mainly through negative regulating the expression of miR-203a [32]. However, whether ANRIL regulated tumorigenesis and progress of hepatoma carcinoma through targeting miR-203a remains unclear. In the present study, it was demonstrated that down-regulation of ANRIL after various treatments led to obvious elevation of miR-203a (Figure 5(A)). Moreover, there was a negative linear correlation between the ANRIL and miR-203a with increase the levels of ANRIL in hepatoma carcinomas resulted in decreased miR-203a expression (Figure 5(B)). Further molecules detection revealed that silencing the expression of ANRIL led to significantly down-regulation of downstream genes of miR-203a, including the Bcl-2, CDK2, c-myc, and p-AKT (Figure 5(C,D)). These results indicated that silencing of the ANRIL levels to inhibit the progress of hepatoma carcinoma was through targeting the miR-203a and its regulated signalling pathways. Additionally, the regulating effect of  $^{D13}$ TBP-3NP on the expressions of miR-203a and its downstream genes were also studied. It was revealed that there was no significant changes for the expressions of miR-203a and its downstream genes was observed after treatment of  $^{D13}$ TBP-3NP, indicating negligible effect of  $^{D13}$ TBP-3 on the mRNAs or proteins activity.

Besides, the effect of  $^{D13}$ TBP-3 on regulation of immunity in tumour microenvironment was subsequently confirmed by

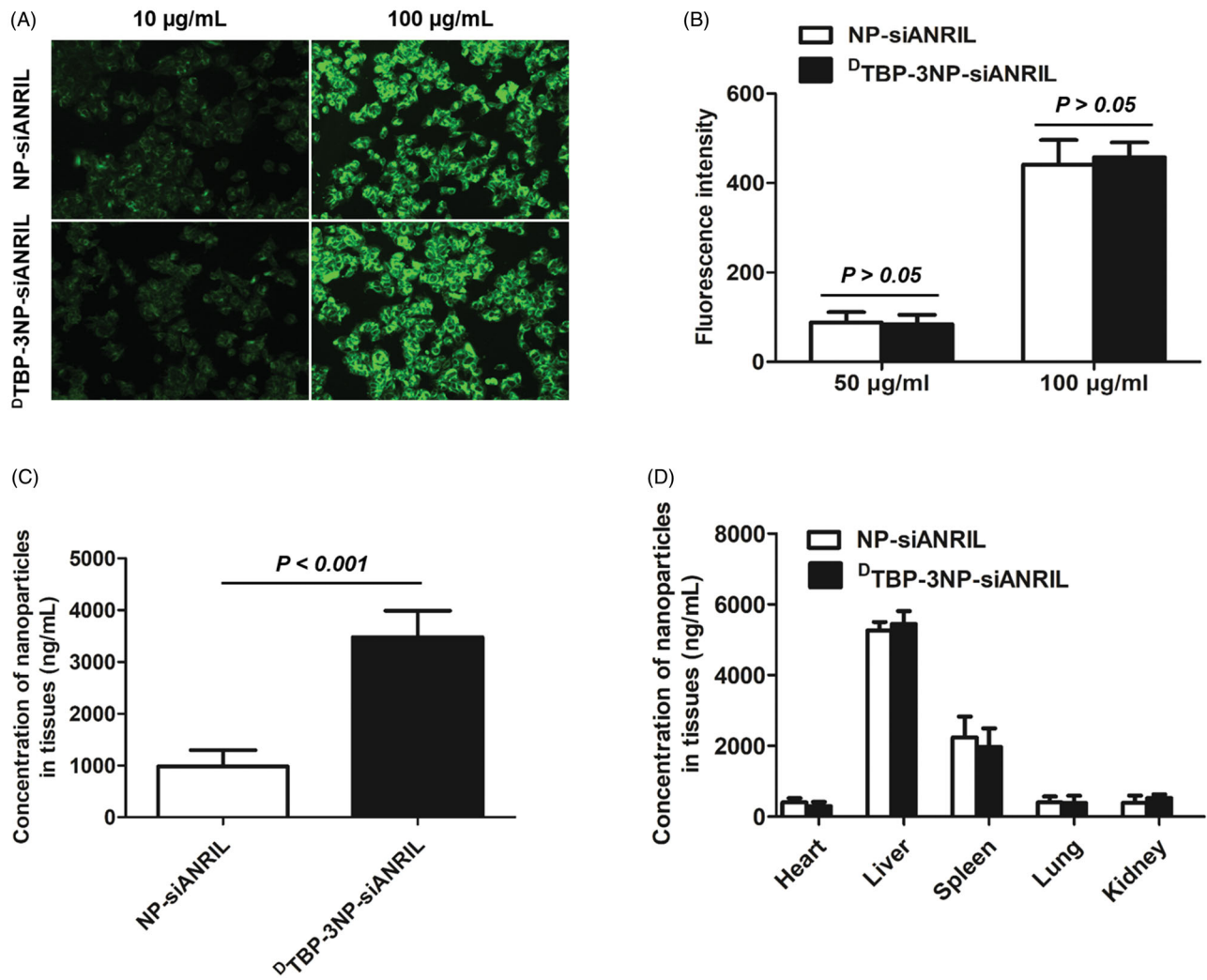


**Figure 3.** Tumour targeting ability of  $^{D2}$ TBP-3NP-siANRIL was respectively determined *in vitro* and *in vivo*. (A) Qualitative analysis of cellular association of FITC-labeled  $^{D2}$ TBP-3NP-siANRIL under the inverted fluorescence microscope and compared with the NP-siANRIL. (B) Quantitative evaluation of cellular association of  $^{D2}$ TBP-3NP-siANRIL and compared with the NP-siANRIL. (C) *In vivo* tumour targeting ability of  $^{D2}$ TBP-3NP-siANRIL was evaluated by determination of the nanoparticle concentrations in tumour tissues. (D) Bio-distribution of  $^{D2}$ TBP-3NP-siANRIL in normal tissues and compared with the un-modified NP-siANRIL.  $p < .001$ , significantly different from the control group.

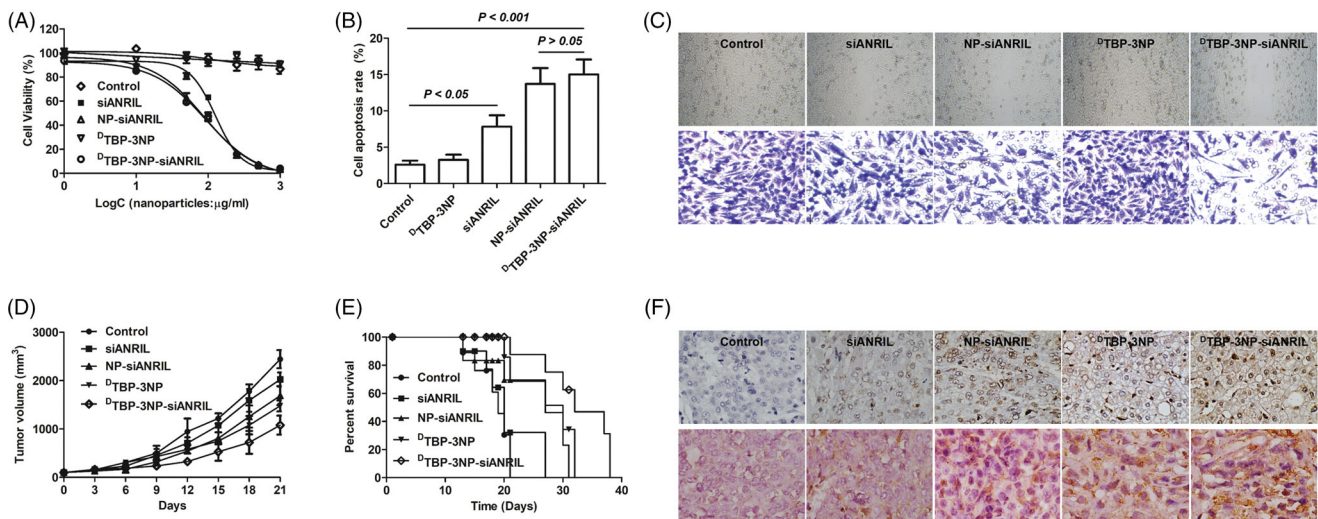


**Figure 4.** Anti-tumour effect of  $^{D2}$ TBP-3NP-siANRIL was evaluated both at cellular level and tumour-bearing animal model. (A) Anti-proliferation of hepatoma carcinoma cells by  $^{D2}$ TBP-3NP-siANRIL was evaluated by determination of cell viability. (B) Apoptosis rate of hepatoma carcinoma cells after treated with different strategies. (C) The lateral migration and vertical mobility of hepatoma carcinoma cells was respectively investigated by wound healing assay and transwell assay. Anti-tumour effect assay *in vivo* was respectively determined by tumour growth (D) and survival experiments (E). (F) TUNEL analysis of cell apoptosis rate (upper) and immunohistochemical evaluation of TIGIT levels (lower) in tumour tissues post various treatments.  $p < .05$ ,  $p < .001$ , significantly different from the control group.

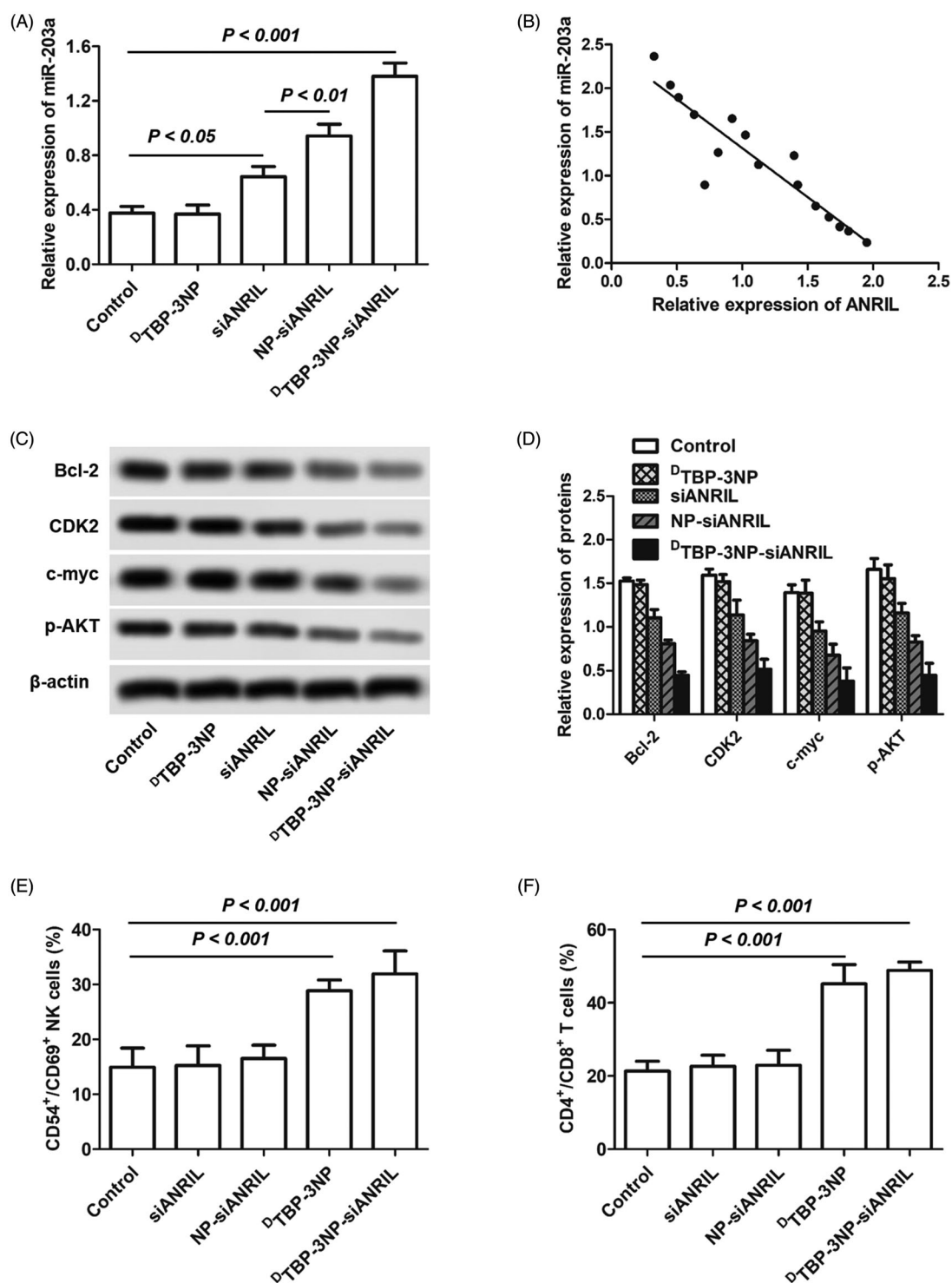


**Figure 5.** Influence of  $D^{12}$ TBP-3NP-siANRIL on cellular signalling and immunity. (A) Expression of miR-203a in hepatoma carcinoma after treated with different strategies detected by RT-qPCR experiments. (B) The correlations between the expressions of ANRIL and miR-203a. (C) The levels of various downstream genes of miR-203a, including the Bcl-2, CDK2, c-myc, and p-AKT in hepatoma carcinoma post various treatments determined by western blot assays. (D) Quantitative evaluation of the levels of Bcl-2, CDK2, c-myc, and p-AKT in hepatoma carcinoma post various treatments determined by RT-qPCR experiments. The percentages of NK cells (E) and T cells (F) in hepatoma carcinoma after different treatments.  $p < .05$ ,  $p < .01$ ,  $p < .001$ , significantly different from the control group.

detection of the percentages of NK cells and T cells after different treatments. As shown in Figure 5(E,F), there was no significant difference on the percentages of NK cells and T cells between the groups of control, siANRIL, and NP-siANRIL, suggested that the ANRIL plays negligible effect on the immunity of hepatoma

carcinoma. In contrast, after treatment of  $D^{12}$ TBP-3NP or  $D^{12}$ TBP-3NP-siANRIL, both the percentages of NK cells and T cells in tumour tissues were dramatically increased, confirmed that the  $D^{12}$ TBP-3 has excellent capacity to activate the immunity of hepatoma carcinoma. Taken together, these results confirmed that  $D^{12}$ TBP-3NP-

siANRIL was able of inhibited the hepatoma carcinoma by simultaneously blocks the TIGIT/PVR for immunotherapy and ANRIL based signalling for gene therapy.

## Conclusion

In the present study, we have developed a novel nano-drug system <sup>D</sup>TBP-3NP-siANRIL for inhibition of hepatoma carcinoma. Importantly, the <sup>D</sup>TBP-3 peptides were conjugated with NP-siANRIL *via* the GSH-sensitive linkage to remain the binding ability of DTBP-3 to TIGIT. Therefore, the developed <sup>D</sup>TBP-3NP-siANRIL was characterised by combining the TIGIT/PVR blocking and ANRIL silencing. It was demonstrated that the levels of TIGIT and ANRIL was significantly increased in hepatoma carcinoma tissues and cells. Although the <sup>D</sup>TBP-3NP-siANRIL exhibited a similar behaviour to the NP-siANRIL, *in vivo* tumour targeting assay exhibited more amount of <sup>D</sup>TBP-3NP-siANRIL was accumulated at tumour sites and resulted in excellent anti-tumour effect than NP-siANRIL. Additionally, it was revealed that treatment of hepatoma carcinoma with <sup>D</sup>TBP-3NP-siANRIL significantly elevated the miR-203a expression and its downstream genes and simultaneously increased the percentages of NK cells and T cells. In a world, the present study demonstrated that the <sup>D</sup>TBP-3NP-siANRIL inhibited hepatoma carcinoma through simultaneously blocks the TIGIT/PVR for immunotherapy and ANRIL based signalling for gene therapy.

## Disclosure statement

The authors declare no competing financial interests.

## References

- [1] Hartke J, Johnson M, Ghabil M. The diagnosis and treatment of hepatocellular carcinoma. *Semin Diagn Pathol.* 2017;34:153–159.
- [2] Clark T, Maximin S, Meier J, et al. Hepatocellular carcinoma: review of epidemiology, screening, imaging diagnosis, response assessment, and treatment. *Curr Probl Diagn Radiol.* 2015;44:479–486.
- [3] Wallace MC, Preen D, Jeffrey GP, et al. The evolving epidemiology of hepatocellular carcinoma: a global perspective. *Expert Rev Gastroenterol Hepatol.* 2015;9:765–779.
- [4] Testino G, Leone S, Patussi V, et al. Hepatocellular carcinoma: diagnosis and proposal of treatment. *Minerva Med.* 2016;107:413–426.
- [5] Zhu Y, Zhang X, Qi L, et al. HULC long noncoding RNA silencing suppresses angiogenesis by regulating ESM-1 via the PI3K/Akt/mTOR signaling pathway in human gliomas. *Oncotarget.* 2016;7:14429–14440.
- [6] Zhou J, Xiang W, Li S, et al. Association between long non-coding RNAs expression and pathogenesis and progression of gliomas. *Oncol Lett.* 2018;15:4070–4078.
- [7] Yu G, Liu G, Yuan D, et al. Long non-coding RNA ANRIL is associated with a poor prognosis of osteosarcoma and promotes tumorigenesis via PI3K/Akt pathway. *J Bone Oncol.* 2018;11:51–55.
- [8] Xie Y, Zhang Y, Du L, et al. Circulating long noncoding RNA act as potential novel biomarkers for diagnosis and prognosis of non-small cell lung cancer. *Mol Oncol.* 2018;12:648–658.
- [9] Bolha L, Ravnik-Glavač M, Glavač D. Long noncoding RNAs as biomarkers in cancer. *Dis Markers.* 2017;2017:7243968.
- [10] Yap KL, Li S, Munoz-Cabello AM, et al. Molecular interplay of the noncoding RNA ANRIL and methylated histone H3 lysine 27 by polycomb CBX7 in transcriptional silencing of INK4a. *Mol Cell.* 2010;38:662–674.
- [11] Wu JH, Tang JM, Li J, et al. Upregulation of SOX2-activated lncRNA ANRIL promotes nasopharyngeal carcinoma cell growth. *Sci Rep.* 2018;8:3333.
- [12] Lin L, Gu ZT, Chen WH, et al. Increased expression of the long non-coding RNA ANRIL promotes lung cancer cell metastasis and correlates with poor prognosis. *Diagn Pathol.* 2015;10:14.
- [13] Poi MJ, Li J, Sborov DW, et al. Polymorphism in ANRIL is associated with relapse in patients with multiple myeloma after autologous stem cell transplant. *Mol Carcinog.* 2017;56:1722–1732.
- [14] Hua L, Wang CY, Yao KH, et al. High expression of long non-coding RNA ANRIL is associated with poor prognosis in hepatocellular carcinoma. *Int J Clin Exp Pathol.* 2015;8:3076–3082.
- [15] Feng M, Xiong G, Cao Z, et al. PD-1/PD-L1 and immunotherapy for pancreatic cancer. *Cancer Lett.* 2017;407:57–65.
- [16] Balar AV, Weber JS. PD-1 and PD-L1 antibodies in cancer: current status and future directions. *Cancer Immunol Immunother.* 2017;66:551–564.
- [17] Sui H, Ma N, Wang Y, et al. Anti-PD-1/PD-L1 therapy for non-small-cell lung cancer: toward personalized medicine and combination strategies. *J Immunol Res.* 2018;2018:6984948.
- [18] Wang Q, Wu X. Primary and acquired resistance to PD-1/PD-L1 blockade in cancer treatment. *Int Immunopharmacol.* 2017;46:210–219.
- [19] Dougall WC, Kurtulus S, Smyth MJ, et al. TIGIT and CD96: new checkpoint receptor targets for cancer immunotherapy. *Immunol Rev.* 2017;276:112–120.
- [20] Stamm H, Wellbrock J, Fiedler W. Interaction of PVR/PVRL2 with TIGIT/DNAM-1 as a novel immune checkpoint axis and therapeutic target in cancer. *Mamm Genome.* 2018;29:694–702.
- [21] Zhou X, Zuo C, Li W, et al. A novel d-peptide identified by mirror-image phage display blocks TIGIT/PVR for cancer immunotherapy. *Angew Chem Int Ed Engl.* 2020.
- [22] Yan S, Ren BY, Shen J. Nanoparticle-mediated double-stranded RNA delivery system: a promising approach for sustainable pest management. *Insect Sci.* 2021;28:21–34.
- [23] Williford JM, Wu J, Ren Y, et al. Recent advances in nanoparticle-mediated siRNA delivery. *Annu Rev Biomed Eng.* 2014;16:347–370.
- [24] Wang W, Xiong W, Wan J, et al. The decrease of PAMAM dendrimer-induced cytotoxicity by PEGylation via attenuation of oxidative stress. *Nanotechnology.* 2009;20:105103.
- [25] Jevprasesphant R, Penny J, Jalal R, et al. The influence of surface modification on the cytotoxicity of PAMAM dendrimers. *Int J Pharm.* 2003;252:263–266.
- [26] Zheng X, Pang X, Yang P, et al. A hybrid siRNA delivery complex for enhanced brain penetration and precise amyloid plaque targeting in Alzheimer's disease mice. *Acta Biomater.* 2017;49:388–401.
- [27] Yang S, Gao H. Nanoparticles for modulating tumor microenvironment to improve drug delivery and tumor therapy. *Pharmacol Res.* 2017;126:97–108.
- [28] Li G, Zhu Y. Effect of lncRNA ANRIL knockdown on proliferation and cisplatin chemoresistance of osteosarcoma cells *in vitro*. *Pathol Res Pract.* 2019;215:931–938.

- [29] Ma Y, Zhang H, Li G, et al. LncRNA ANRIL promotes cell growth, migration and invasion of hepatocellular carcinoma cells via sponging miR-144. *Anticancer Drugs*. 2019;30: 1013–1021.
- [30] Kulkarni SA, Feng SS. Effects of particle size and surface modification on cellular uptake and biodistribution of polymeric nanoparticles for drug delivery. *Pharm Res*. 2013;30: 2512–2522.
- [31] Ernsting MJ, Murakami M, Roy A, et al. Factors controlling the pharmacokinetics, biodistribution and intratumoral penetration of nanoparticles. *J Control Release*. 2013;172: 782–794.
- [32] Dai W, Tian C, Jin S. Effect of lncRNA ANRIL silencing on anoikis and cell cycle in human glioma via microRNA-203a. *Onco Targets Ther*. 2018;11: 5103–5109.